Two-dimensional atom localization via probe absorption in a four-level atomic system*

Wang Zhi-Ping(王志平)[a)†], Ge Qiang(葛 强)[a)b)], Ruan Yu-Hua(阮于华)[a)], and Yu Ben-Li(俞本立)[a)]

[a)] *Key Laboratory of Opto-Electronic Information Acquisition and Manipulation of Ministry of Education, Anhui University, Hefei* 230601, *China*
[b)] *School of Mathematics and Physics, Anhui Polytechnic University, Wuhu* 241000, *China*

(Received 05 September 2012; revised manuscript received 21 November 2012)

We have investigated the two-dimensional (2D) atom localization via probe absorption in a coherently driven four-level atomic system by means of a radio-frequency field driving a hyperfine transition. It is found that the detecting probability and precision of 2D atom localization can be significantly improved via adjusting the system parameters. As a result, our scheme may be helpful in laser cooling or the atom nano-lithography via atom localization.

Keywords: two-dimensional (2D) atom localization, probe absorption, four-level atomic system

PACS: 42.50.Gy **DOI:** 10.1088/1674-1056/22/7/074203

1. Introduction

During the past few years, the precision position measurement of an atom has been a subject of many recent studies because of its wide potential applications in trapping of neutral atoms, laser cooling,[1] and atom nano-lithography,[2] etc. Earlier studies[3–5] in the localization included the measurement of the phase shift of either the standing wave or the atomic dipole due to the interaction of the atom with the standing-wave field, the entanglement between the position of atom and its internal states, and resonance imaging methods. It is well known that quantum coherence and interference can give rise to some interesting phenomena, such as, electromagnetically induced transparency,[6–8] lasing without inversion[9,10] spontaneously generated coherence,[11,12] multi-wave mixing,[13–15] enhancing Kerr nonlinearity,[16,17] optical soliton,[18–20] and so on. Based on the atomic coherence and quantum interference, many schemes have been proposed for atom localization. For example, Qamar *et al.*[21] suggested the atom localization based on resonance fluorescence in a two-level system driven by a strong standing-wave field. Paspalakis and Knight proposed a quantum-interference-induced sub-wavelength atomic localization a three-level Λ-type atom interacting with a classical standing-wave field and a weak probe laser field, and they found that the atomic position with high precision can be achieved via the measurement of the upper-state atom population.[22] Recently, in a four-level atomic system with a closed-loop configuration, Zubairy and coworkers shown two schemes[23,24] that the phase of the standing-wave driving field plays an important role in reducing the number of localization peaks from the usual four to two, leading to sub-half-wavelength atom localization. At the same time, Gong *et al.*[25,26] presented two schemes based on double-dark resonance effects and demonstrated that the atom can be localized at the nodes of the standing-wave field, and the detecting probability can be increased to 1/2. Interestingly, instead of the measurement of the population in the excited state, the detection of the population in the ground state coupled to the standing-wave field leads to only two localization peaks in a unit wavelength region. This was shown by Agarwal and Kapale,[27] who put emphasis on the momentum distribution and the role of the ratio of the intensities of the coupling and probe fields. Of course, some relative schemes for realizing 1D atom localization were also studied.[28–32]

On the other hand, two-dimensional (2D) atom localization has also been extensively studied in the multilevel atomic system. The studies show that one can control 2D atom localization via the measurement of the upper-state or any ground-state population of the four-level atom,[33] via interacting double-dark resonances,[34] via controlled spontaneous emission,[35–38] or via the probe absorption spectrum.[39–41] In this work, we investigate the 2D atom localization behaviors in a four-level atomic system via controlled probe absorption spectrum. It is found that the detecting probability and precision of 2D atom localization behaviors can be significantly improved due to the quantum interference generated by the laser and radio-frequency fields. Our work is mainly based on Refs. [20]–[44], however, which is drastically different from those works. First, the present scheme is based on the probe absorption measurement, and the absorption measurement is much easier to carry out in a laboratory compared with the measurement of spontaneous emission.[35–38] Second, a few works have discussed the efficient 2D atom localization be-

*Project supported by the National Natural Science Foundation of China (Grant No. 11205001), the National Basic Research Program of China (Grant No. 2010CB234607), and the Postdoctoral Science Foundation of Anhui University, China.

†Corresponding author. E-mail: zhipwang@126.com

© 2013 Chinese Physical Society and IOP Publishing Ltd

haviors via phase-dependent probe absorption spectrum,[39,40] however, five fields are used to control the 2D atom localization behaviors. It is well known that the external fields are less convenient for experimental realization, which may be the serious reason to sophisticate the experimental setup. Unlike those works, only four fields are applied in present scheme, which make our scheme much more convenient in experimental realization. Third, the 2D atom localization patterns reveal that the probability of finding an atom within the subwavelength domain of the standing waves can arrive at 1/2, which is increased by a factor of 2 compared with the previous proposed schemes.[33,35,41] The rest of the paper is organized as follows: in Section 2, we present the theoretical model and establish the corresponding equations. The possible experimental realization and numerical results are shown in Sections 3 and 4, respectively. In Section 5, some simple conclusions are given.

2. The model and dynamic equations

We consider a four-level atomic system as shown in Fig. 1(a). This system has one stable ground state $|1\rangle$, one intermediate level $|2\rangle$ and two-folded levels $|3\rangle$ and $|4\rangle$. The composition of two orthogonal standing-wave fields $\Omega_{\rm s}(x,y)$ are applied to the transition $|3\rangle \leftrightarrow |2\rangle$. The Rabi frequencie is dependent on the position and defined by $2\Omega_{\rm s}(x,y) = 2\Omega_{xy}[\sin(kx)+\sin(ky)]$ (frequency ω_{xy}). We apply a weak probe field with Rabi frequency $2\Omega_{\rm p}$ (frequency $\omega_{\rm p}$) to couple the transition $|2\rangle \leftrightarrow |1\rangle$. An assisting rf driving field with Larmor frequency $2\Omega_{\rm rf}$ (frequency $\omega_{\rm rf}$) is used to couple upper two-folded levels.

We assume that the center-of-mass position of the atom is nearly constant along the direction of the laser waves and neglect the kinetic part of the atom from the Hamiltonian in the Raman–Nath approximation. Note that during the interaction, the atomic position does not change directly and our localization scheme only influences the internal states of the atom. Then, in the interaction picture and under the rotating-wave approximation, the Hamiltonian of this system is given as follows ($\hbar = 1$):

$$\begin{aligned} H_{\rm int} = {} & \Delta_{\rm p}|2\rangle\langle 2| + \left(\Delta_{\rm p}+\Delta_{xy}\right)|3\rangle\langle 3| + \left(\Delta_{\rm p}+\Delta_{xy}+\Delta_{\rm rf}\right)|4\rangle\langle 4| \\ & - \left(\Omega_{\rm p}|2\rangle\langle 1| + \Omega_{\rm s}(x,y)|3\rangle\langle 2| + \Omega_{\rm rf}|4\rangle\langle 3| + {\rm H.c.}\right), \quad (1) \end{aligned}$$

where $\Delta_{\rm p} = \omega_{21} - \omega_{\rm p}$, $\Delta_{xy} = \omega_{32} - \omega_{xy}$, and $\Delta_{\rm rf} = \omega_{43} - \omega_{\rm rf}$ are the detunings of the probe field, the standing-wave field and the rf field, respectively, $2\Omega_{xy} = E_{xy}\mu_{32}/\hbar$, $2\Omega_{\rm p} = E_{\rm p}\mu_{21}/\hbar$, and $2\Omega_{\rm rf} = E_{\rm rf}\mu_{42}/\hbar$ are the Rabi and Larmor frequencies of the optical fields. μ_{mn} $(m,n = 1,2,3,4)$ are the dipole matrix elements and E_j $(j = xy, {\rm rf}, {\rm p})$ are the slowly varying amplitudes of the optical fields. The ω_{43}, ω_{32}, and ω_{21} are resonant frequencies which associate with the corresponding transitions $|4\rangle \leftrightarrow |3\rangle$, $|3\rangle \leftrightarrow |2\rangle$, and $|2\rangle \leftrightarrow |1\rangle$.

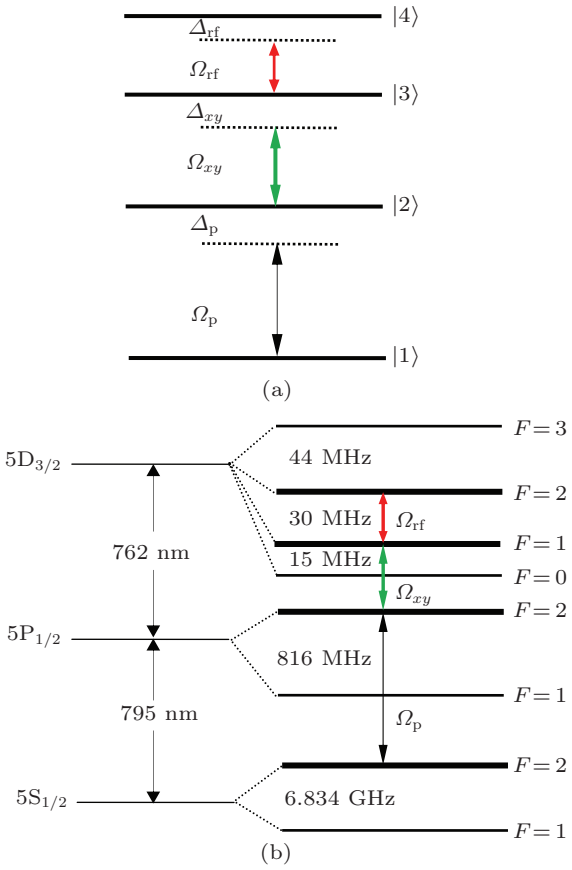


Fig. 1. (color online) (a) Schematic diagram of the four-level atomic system. (b) Specific case for a ^{87}Rb atom as an example.

The dynamics of the system can be described using the density-matrix approach as

$$\frac{\partial \rho}{\partial t} = -\frac{\rm i}{\hbar}[H,\rho] + L\rho, \quad (2)$$

and then we have

$$\frac{\partial \rho_{11}}{\partial t} = \gamma_2\rho_{22} + {\rm i}\Omega_{\rm p}^*\rho_{21} - {\rm i}\Omega_{\rm p}\rho_{12}, \quad (3a)$$

$$\begin{aligned} \frac{\partial \rho_{22}}{\partial t} = {} & -\gamma_2\rho_{22} + \gamma_3\rho_{33} + \gamma_4\rho_{44} - {\rm i}\Omega_{\rm p}^*\rho_{21} \\ & + {\rm i}\Omega_{\rm p}\rho_{12} + {\rm i}\Omega_{\rm s}^*(x,y)\rho_{32} - {\rm i}\Omega_{\rm s}(x,y)\rho_{23}, \quad (3b) \end{aligned}$$

$$\begin{aligned} \frac{\partial \rho_{33}}{\partial t} = {} & -\gamma_3\rho_{33} - {\rm i}\Omega_{\rm s}^*(x,y)\rho_{32} + {\rm i}\Omega_{\rm s}(x,y)\rho_{23} \\ & - {\rm i}\Omega_{\rm rf}\rho_{34} + {\rm i}\Omega_{\rm rf}^*\rho_{43}, \quad (3c) \end{aligned}$$

$$\frac{\partial \rho_{44}}{\partial t} = -\gamma_4\rho_{44} - {\rm i}\Omega_{\rm rf}^*\rho_{43} + {\rm i}\Omega_{\rm rf}\rho_{34}, \quad (3d)$$

$$\begin{aligned} \frac{\partial \rho_{21}}{\partial t} = {} & -\left(\frac{\gamma_2}{2} + {\rm i}\Delta_{\rm p}\right)\rho_{21} + {\rm i}\Omega_{\rm p}(\rho_{11}-\rho_{22}) \\ & + {\rm i}\Omega_{\rm s}^*(x,y)\rho_{31}, \quad (3e) \end{aligned}$$

$$\begin{aligned} \frac{\partial \rho_{31}}{\partial t} = {} & -\left[\frac{\gamma_3}{2} + {\rm i}\left(\Delta_{\rm p}+\Delta_{xy}\right)\right]\rho_{31} \\ & + {\rm i}\Omega_{\rm rf}^*\rho_{41} - {\rm i}\Omega_{\rm p}\rho_{32} + {\rm i}\Omega_{\rm s}(x,y)\rho_{21}, \quad (3f) \end{aligned}$$

$$\frac{\partial \rho_{41}}{\partial t} = -\left[\frac{\gamma_4}{2} + {\rm i}\left(\Delta_{\rm p}+\Delta_{xy}+\Delta_{\rm rf}\right)\right]\rho_{41}$$

$$+\mathrm{i}\Omega_{\mathrm{rf}}\rho_{31}-\mathrm{i}\Omega_{\mathrm{p}}\rho_{42}, \tag{3g}$$

$$\frac{\partial\rho_{32}}{\partial t}=-\left(\frac{\gamma_2+\gamma_3}{2}+\mathrm{i}\Delta_{xy}\right)\rho_{32}+\mathrm{i}\Omega_{\mathrm{rf}}^{*}\rho_{42} -\mathrm{i}\Omega_{\mathrm{p}}^{*}\rho_{31}+\mathrm{i}\Omega_{\mathrm{s}}(x,y)(\rho_{22}-\rho_{33}), \tag{3h}$$

$$\frac{\partial\rho_{42}}{\partial t}=-\left[\frac{\gamma_2+\gamma_4}{2}+\mathrm{i}(\Delta_{xy}+\Delta_{\mathrm{rf}})\right]\rho_{42} +\mathrm{i}\Omega_{\mathrm{rf}}\rho_{32}-\mathrm{i}\Omega_{\mathrm{p}}^{*}\rho_{41}-\mathrm{i}\Omega_{\mathrm{s}}(x,y)\rho_{43}, \tag{3i}$$

$$\frac{\partial\rho_{43}}{\partial t}=-\left(\frac{\gamma_3+\gamma_4}{2}+\mathrm{i}\Delta_{\mathrm{rf}}\right)\rho_{43} +\mathrm{i}\Omega_{\mathrm{rf}}(\rho_{33}-\rho_{44})-\mathrm{i}\Omega_{\mathrm{s}}^{*}(x,y)\rho_{42}, \tag{3j}$$

where γ_2, γ_3, and γ_4 are added phenomenologically to describe the decay rates from the excited state $|2\rangle$ to the ground state $|1\rangle$, from the excited state $|3\rangle$ to the excited state $|2\rangle$, and from the excited state $|4\rangle$ to the excited state $|2\rangle$, respectively.

In the limit of the weak-probe field, we take the magnitude of the probe field Rabi frequency Ω_{p} to be sufficiently small as compared with Rabi frequencies of the standing waves Ω_{xy} and the rf field Larmor frequencies Ω_{rf}. Therefore, we can take almost all atoms remain in the level $|1\rangle$ initially during the atom-field interaction

$$\rho_{11}^{(0)}=1,\ \rho_{mn}^{(0)}=0,\ (m\neq 1, n\neq 1). \tag{4}$$

Considering all orders of the standing-wave fields, and the linear order of the weak probe field, we only need Eqs. (3e), (3f), and (3g) to determine the expression of susceptibility. The equations can be written simply as

$$\frac{\partial\rho_{21}^{(1)}}{\partial t}=-\left(\frac{\gamma_2}{2}+\mathrm{i}\Delta_{\mathrm{p}}\right)\rho_{21}^{(1)}+\mathrm{i}\Omega_{\mathrm{p}}+\mathrm{i}\Omega_{\mathrm{s}}(x,y)\rho_{31}^{(1)},$$

$$\frac{\partial\rho_{31}^{(1)}}{\partial t}=-\left[\frac{\gamma_3}{2}+\mathrm{i}\left(\Delta_{\mathrm{p}}+\Delta_{xy}\right)\right]\rho_{31}^{(1)} +\mathrm{i}\Omega_{\mathrm{rf}}\rho_{41}^{(1)}+\mathrm{i}\Omega_{\mathrm{s}}(x,y)\rho_{21}^{(1)},$$

$$\frac{\partial\rho_{41}^{(1)}}{\partial t}=-\left[\frac{\gamma_4}{2}+\mathrm{i}\left(\Delta_{\mathrm{p}}+\Delta_{xy}+\Delta_{\mathrm{rf}}\right)\right]\rho_{41}^{(1)}+\mathrm{i}\Omega_{\mathrm{rf}}\rho_{31}^{(1)}.$$

We can obtain straightforwardly the susceptibility at the probe frequency written as

$$\chi_{\mathrm{p}}=\frac{N|\mu_{21}|^2}{2\varepsilon_0\hbar\Omega_{\mathrm{p}}}\rho_{21}^{(1)}=\frac{\mathbb{N}}{\Omega_{\mathrm{p}}}\rho_{21}^{(1)}, \tag{5}$$

where

$$\mathbb{N}=\frac{N|\mu_{21}|^2}{\varepsilon_0\hbar},$$

$$\rho_{21}^{(1)}=\mathrm{i}\Omega_{\mathrm{p}}\frac{\alpha_3\alpha_4+\Omega_{\mathrm{rf}}^2}{\Omega_{\mathrm{rf}}^2\alpha_2+\Omega_{\mathrm{s}}^2(x,y)\alpha_4+\alpha_2\alpha_3\alpha_4},$$

with $\alpha_2=\gamma_2/2+\mathrm{i}\Delta_{\mathrm{p}}$, $\alpha_3=\gamma_3/2+\mathrm{i}\left(\Delta_{\mathrm{p}}+\Delta_{xy}\right)$, and $\alpha_4=\gamma_4/2+\mathrm{i}\left(\Delta_{\mathrm{p}}+\Delta_{xy}+\Delta_{\mathrm{rf}}\right)$. N is the atom number density in the medium.

It is well known that the imaginary part of the susceptibility accounts for absorption, based on Eqs. (3) and (5), which can be expressed as follows (keep $\mathbb{N}=1$):

$$\mathrm{Im}(\chi_{\mathrm{p}})\simeq\mathrm{Im}\left(\frac{\rho_{21}^{(1)}}{\Omega_{\mathrm{p}}}\right)=\mathrm{Im}\frac{\alpha_3\alpha_4+\Omega_{\mathrm{rf}}^2}{\Omega_{\mathrm{rf}}^2\alpha_2+\Omega_{\mathrm{s}}^2(x,y)\alpha_4+\alpha_2\alpha_3\alpha_4}\mathrm{i} =\frac{\mathbb{R}\left(\gamma_3\gamma_4/4-\Delta_3\Delta_4+\Omega_{\mathrm{rf}}^2\right)-\mathbb{Z}\left(\Delta_3\gamma_4/2+\Delta_4\gamma_3/2\right)}{\mathbb{R}^2+\mathbb{Z}^2}, \tag{6}$$

where

$$\mathbb{R}=\frac{1}{2}\left(\gamma_2\Omega_{\mathrm{rf}}^2+\gamma_4\Omega_{\mathrm{s}}^2(x,y)-\Delta_{\mathrm{p}}\Delta_3\gamma_4 -\gamma_2\Delta_3\Delta_4-\gamma_3\Delta_{\mathrm{p}}\Delta_4+\frac{\gamma_2\gamma_3\gamma_4}{4}\right),$$

$$\mathbb{Z}=\Delta_{\mathrm{p}}\Omega_{\mathrm{rf}}^2+\Delta_4\Omega_{\mathrm{s}}^2(x,y)-\Delta_{\mathrm{p}}\Delta_3\Delta_4 +\frac{1}{4}\left(\gamma_2\gamma_4\Delta_3+\gamma_3\gamma_4\Delta_{\mathrm{p}}+\gamma_2\gamma_3\Delta_4\right),$$

$$\Delta_3=\Delta_{\mathrm{p}}+\Delta_{xy},$$

$$\Delta_4=\Delta_{\mathrm{p}}+\Delta_{xy}+\Delta_{\mathrm{rf}}.$$

Equation (6) exhibits that $\mathrm{Im}(\chi_{\mathrm{p}})$ is dependent on the positions (x,y), the detunings of optical fields Δ_{p}, Δ_{xy}, and Δ_{rf}, as well as the Rabi frequencies $\Omega_{\mathrm{s}}(x,y)$ and Ω_{rf}. It is, in principle, possible to obtain the information about the conditional position probability distribution of the atom. Thus, the problem reduces to determining probe absorption $\mathrm{Im}(\rho_{21}^{(1)}/\Omega_{\mathrm{p}})$, the measurement of such a position-dependent quantity can provide information on the atomic position and lead to 2D atom localization.

3. Possible experimental realization

Before showing our results, let us briefly discuss the possible experimental realization of our proposed scheme for the present study, which are given as follows.

(i) We consider, for instance, the cold atoms ^{87}Rb (nuclear spin $I=3/2$) on the 5S–5P–5D transitions as a possible candidate.[42] The detailed coupling diagram is shown in Fig. 1(b). The experimental system for this atomic scheme can be realized by the ^{87}Rb atom with $|5\mathrm{S}_{1/2},F=2\rangle$, $|5\mathrm{P}_{1/2},F=2\rangle$, $|5\mathrm{D}_{3/2},F=1\rangle$, and $|5\mathrm{D}_{3/2},F=2\rangle$ behaving the $|1\rangle$, $|2\rangle$, $|3\rangle$, and $|4\rangle$ state labels, respectively.

(ii) Based on Ref. [43], we found the decay rates from the excited state $|2\rangle$ to the ground state $|1\rangle$, from the excited state $|3\rangle$ to the excited state $|2\rangle$, and from the excited state $|4\rangle$ to the excited state $|2\rangle$ are $\gamma_1\simeq 5.3$ MHz, $\gamma_2\simeq 0.67$ MHz, and $\gamma_3\simeq 0.67$ MHz, respectively. It should be also pointed out that the decay rates from states $|4\rangle$ and $|3\rangle$ to state $|1\rangle$ are zero, because these transitions are non-dipole allowed in our considered model. The relaxation rate of coherence between states $|4\rangle$ and $|3\rangle$ is negligible and thus can be safely neglected.

(iii) We consider that an atom, moving along the z axis, passes through the intersectant region of two orthogonal standing-wave laser fields, which are respectively aligned

along the x and y axes. The weak probe field propagates along the positive z direction in the x–z plane, whereas the rf field propagates along the negative z direction in the x–z plane. The composition of two orthogonal standing waves can be obtained by combining four identical beams, where a pair of identical beams propagate along the positive and negative x directions in the x–y plane while another pair of identical beams propagate along the positive and negative y directions in the x–y plane. A pair of Helmholtz coils produce a MHz rf radiation driving the magnetic dipole transition.[44] The probe absorption observed at appropriate frequencies is position dependent. Such position-dependent probe absorption can be reflected by a standard spectroscopic method or the heterodyne measurement of fluorescence images, which may be realized via the experiment proposed in Ref. [32].

4. Numerical results

Now, we analyze the conditional position probability distribution of the atom via a few numerical calculations based on the probe absorption $\mathrm{Im}(\chi_\mathrm{p})$ in Eq. (6), and then address how the system parameters can be used to achieve 2D atom localization by controlled probe absorption.

The probe absorption $\mathrm{Im}(\chi_\mathrm{p})$ versus the positions (kx, ky) for different values of the probe detuning is plotted in Fig. 2. As can be seen, the probe detuning affects the spatial pattern and resolution of the atom localization. On the condition of $\Delta_\mathrm{p} = 4\gamma$, the probe absorption is distributed in four different quadrants (Fig. 2(a)). When the detuning is tuned to $\Delta_\mathrm{p} = 10\gamma$, the localization peaks display two crater-like patterns, and the atom is localized at these circles (Fig. 2(b)). With the increase of the detuning to further higher values (i.e. $\Delta_\mathrm{p} = 12\gamma$ and 13γ in Figs. 2(c) and 2(d)), the spatial distribution of the probe absorption exhibits two spike-like patterns. From the discussions above, it is obvious that there is a strong correlation between the probe detuning and the position of the atom. The measurement of a particular frequency detuning corresponds to the localization of the atom within a subwavelength region of the standing-wave field.

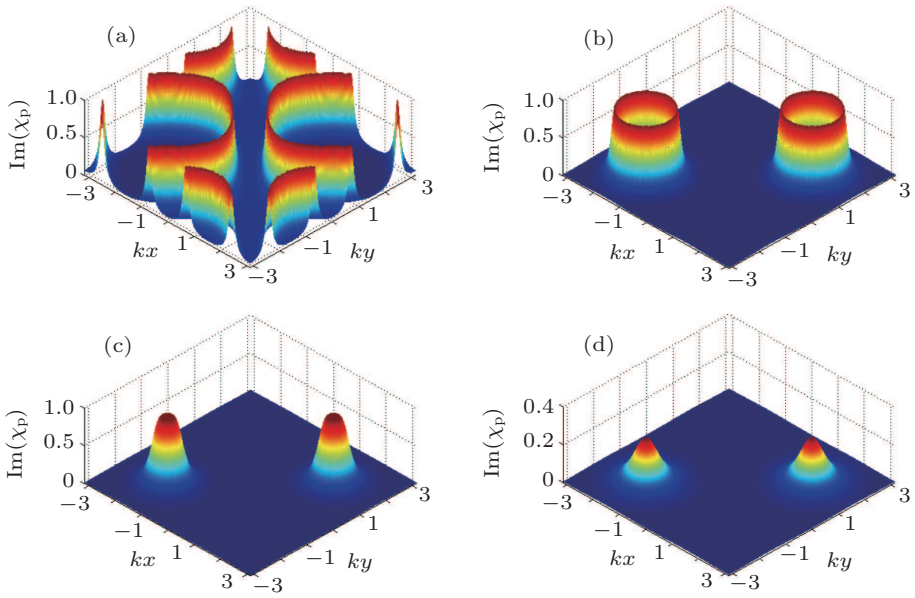


Fig. 2. (color online) Probe absorption spectrum $\mathrm{Im}(\chi_\mathrm{p})$ versus positions kx ($-\pi \leqslant kx \leqslant \pi$) and ky ($-\pi \leqslant ky \leqslant \pi$) for four different frequency detunings of probe field Δ_p: (a) $\Delta_\mathrm{p} = 4\gamma$, (b) $\Delta_\mathrm{p} = 10\gamma$, (c) $\Delta_\mathrm{p} = 12\gamma$, and (d) $\Delta_\mathrm{p} = 13\gamma$. The other parameters are $\Omega_{xy} = 6\gamma$, $\Omega_\mathrm{rf} = \gamma$, $\Delta_\mathrm{rf} = \Delta_{xy} = 0$, $\gamma_3 = \gamma_4 = 0.25\gamma$, and $\gamma_2 = 2\gamma$.

In Fig. 3, we study the effect of the intensity of the rf field on the spatial distribution of the 2D atom localization. For a small intensity of the rf field, i.e., $\Omega_\mathrm{rf} = \gamma$, the probe absorption $\mathrm{Im}(\chi_\mathrm{p})$ shows two spike-like patterns (Fig. 3(a)). When the rf field is adjusted to $\Omega_\mathrm{rf} = 3\gamma$, the two spike-like patterns become two crater-like patterns, as shown in Fig. 3(b). With further increase of Ω_rf ($\Omega_\mathrm{rf} = 6\gamma$), the spatial distribution of the probe absorption does not change, but the caliber of every crater-like pattern becomes wide (Fig. 3(c)). In such a case, we can obtain a high-precision and high-resolution 2D atom localization which can be attributed to the quantum interference effect induced by the rf field. However, on the condition of $\Omega_\mathrm{rf} = 12\gamma$, the probe absorption is distributed in four different quadrants (Fig. 3(d)), which implies that too strong rf field will bring a destructive effect to the precision and spatial distribution of 2D atom localization.

Finally, the influence of frequency detuning of the standing-wave fields Δ_{xy} on 2D probe absorption is exhibited in Fig. 4. Clearly, one can see that the spatial distribution of the probe absorption $\mathrm{Im}(\chi_\mathrm{p})$ is very sensitive to the frequency de-

tuning of the standing-wave fields. It is interesting to see from Figs. 4(a) and 4(b) that the probe absorption $\mathrm{Im}(\chi_p)$ displays two crater-like patterns when the detuning Δ_{xy} is negative, and the caliber of every crater-like pattern becomes wide with the increase of the negative frequency detuning of the standing-wave fields. However, the probe absorption $\mathrm{Im}(\chi_p)$ shows two spike-like patterns when the detuning Δ_{xy} is positive. According to the above discussions, one can conclude that the frequency detuning of the composite standing-wave fields plays an important role in realizing 2D atom localization.

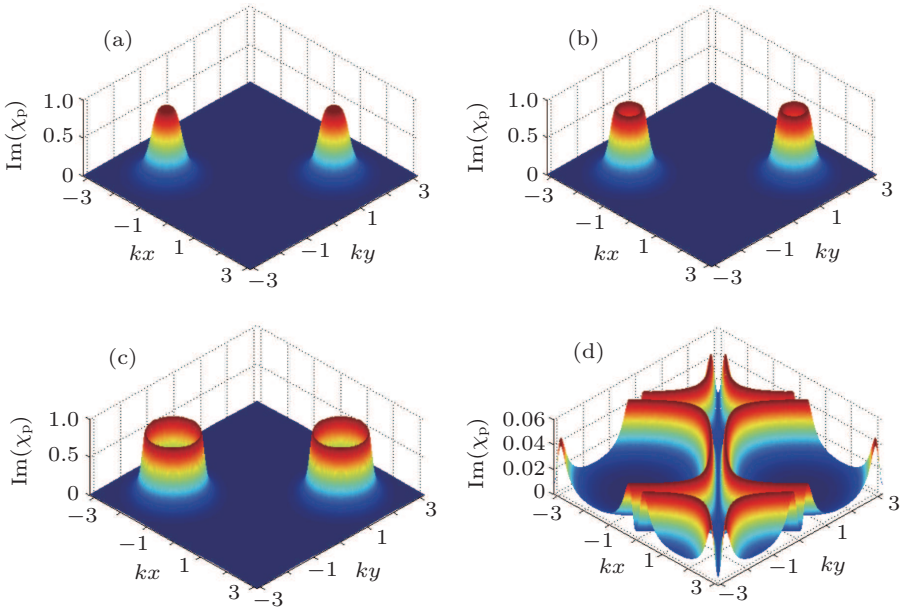


Fig. 3. (color online) Probe absorption spectrum $\mathrm{Im}(\chi_p)$ versus positions kx ($-\pi \leqslant kx \leqslant \pi$) and ky ($-\pi \leqslant ky \leqslant \pi$) for four different intensities of the rf field Ω_{rf}: (a) $\Omega_{rf} = \gamma$, (b) $\Omega_{rf} = 3\gamma$, (c) $\Omega_{rf} = 6\gamma$, and (d) $\Omega_{rf} = 12\gamma$. The other parameters are $\Omega_{xy} = 6\gamma$, $\Delta_p = 12\gamma$, $\Delta_{rf} = \Delta_{xy} = 0$, $\gamma_3 = \gamma_4 = 0.25\gamma$, and $\gamma_2 = 2\gamma$.

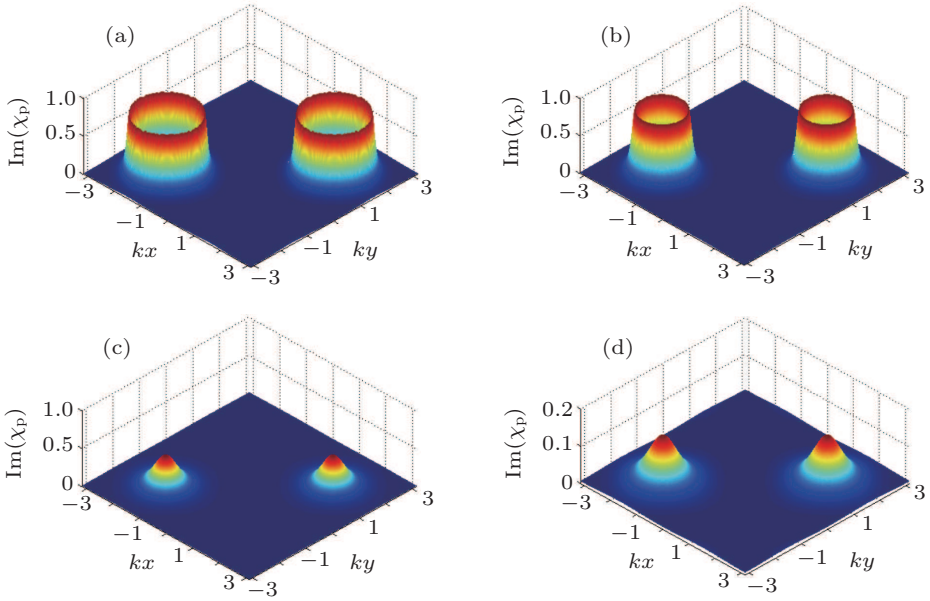


Fig. 4. (color online) Probe absorption spectrum $\mathrm{Im}(\chi_p)$ versus positions kx ($-\pi \leqslant kx \leqslant \pi$) and ky ($-\pi \leqslant ky \leqslant \pi$) for four different frequency detunings of the composite standing-wave fields Δ_{xy}: (a) $\Delta_{xy} = -4\gamma$, (b) $\Delta_{xy} = -2\gamma$, (c) $\Delta_{xy} = 2\gamma$, and (d) $\Delta_{xy} = 4\gamma$. The other parameters are $\Omega_{xy} = 6\gamma$, $\Omega_{rf} = 3\gamma$, $\Delta_p = 12\gamma$, $\Delta_{rf} = 0$, $\gamma_3 = \gamma_4 = 0.25\gamma$, and $\gamma_2 = 2\gamma$.

5. Conclusion

To sum up, we investigated the 2D atom localization via probe absorption in a coherently driven four-level atomic system by means of a radio-frequency field driving a hyperfine transition. It is found that the detecting probability and the precision of 2D atom localization behaviors can be significantly improved via adjusting the system parameters, and the maxi-

mal probability of finding an atom within the sub-wavelength domain of the standing waves can reach 1/2, which is increased by a factor of 2 compared with the previous proposed schemes.[33,35,41] As a result, our scheme may be helpful in laser cooling or atom nano-lithography via atom localization.

References

[1] Phillips W D 1998 *Rev. Mod. Phys.* **70** 721
[2] Johnson K S, Thywissen J H, Dekker N H, Berggren K K, Chu A P, Younkin R and Prentiss M 1998 *Science* **280** 1583
[3] Storey P, Collett M and Walls D F 1992 *Phys. Rev. Lett.* **68** 472
[4] Kunze S, Dieckmann K and Rempe G 1997 *Phys. Rev. Lett.* **78** 2038
[5] Thomas J E and Wang L J 1995 *Phys. Rep.* **262** 311
[6] Harris S E 1997 *Phys. Today* **50** 36
[7] Fleischhauer M, Imamoğlu A and Marangos J P 2005 *Rev. Mod. Phys.* **77** 633
[8] Gao J, Wang J, Zhang T C, Wang J M and Yang B D 2011 *Acta Phys. Sin.* **60** 114207
[9] Harris S E 1989 *Phys. Rev. Lett.* **62** 1033 (in Chinese)
[10] Wu J H, Wang D P, Zhang H F, Xiao Z H and Gao J Y 2003 *Chin. Phys* **12** 39
[11] Zhu S Y, Chen H and Huang H 1997 *Phys. Rev. Lett.* **79** 205
[12] Paspalakis E, Keitel C H and Knight P L 1998 *Phys. Rev. A* **58** 4868
[13] Yang X X and Wu Y 2003 *Chin. Phys. Lett.* **20** 1736
[14] Wu Y and Yang X 2004 *Phys. Rev. A* **70** 053818
[15] Zhang Y, Khadka U, Anderson B and Xiao M 2009 *Phys. Rev. Lett.* **102** 013601
[16] Wang H, Goorskey D and Xiao M 2001 *Phys. Rev. Lett.* **87** 073601
[17] Niu Y P and Gong S Q 2006 *Phys. Rev. A* **73** 053811
[18] Wu Y and Deng L 2004 *Opt. Lett.* **29** 2064
[19] Wu Y and Deng L 2004 *Phys. Rev. Lett.* **93** 143904
[20] Yang W X, Chen A X, Lee R K and Wu Y 2011 *Phys. Rev. A* **84** 013835
[21] Qamar S, Zhu S Y and Zubairy M S 2000 *Phys. Rev. A* **61** 063806
[22] Paspalakis E and Knight P L 2001 *Phys. Rev. A* **63** 065802
[23] Sahrai M, Tajalli H, Kapale K T and Zubairy M S 2005 *Phys. Rev. A* **72** 013820
[24] Kapale K T and Zubairy M S 2006 *Phys. Rev. A* **73** 023813
[25] Liu C P, Gong S Q, Cheng D C, Fan X J and Xu Z Z 2006 *Phys. Rev. A* **73** 025801
[26] Cheng D, Niu Y, Li R and Gong S 2006 *J. Opt. Soc. Am. B* **23** 2180
[27] Agarwal G S and Kapale K T 2006 *J. Phys. B* **39** 3437
[28] Macovei M, Evers J, Keitel C H and Zubairy M S 2007 *Phys. Rev. A* **75** 033801
[29] Xu J and Hu X M 2007 *Phys. Rev. A* **76** 013830
[30] Qamar S, Mehmood A and Qamar S 2009 *Phys. Rev. A* **79** 033848
[31] Wang Z and Jiang J 2010 *Rev. Lett. A* **374** 4853
[32] Proite N A, Simmons Z J and Yavuz D D 2011 *Phys. Rev. A* **83** 041803
[33] Ivanov V and Rozhdestvensky Y 2010 *Phys. Rev. A* **81** 033809
[34] Wan R G, Kou J, Jiang L, Jiang Y and Gao J Y 2011 *J. Opt. Soc. Am. B* **28** 622
[35] Ding C, Li J, Zhan Z and Yang X 2011 *Phys. Rev. A* **83** 063834
[36] Wan R G, Kou J, Jiang L, Jiang Y and Gao J Y 2011 *J. Opt. Soc. Am. B* **28** 10
[37] Wang Z, Yu B, Zhu J, Cao Z, Zhen S, Wu X and Xu F 2012 *Ann. Phys.* **327** 1132
[38] Ding C, Li J, Yu R, Hao X and Wu Y 2012 *Opt. Express* **20** 7870
[39] Li J, Yu R, Liu M, Ding C and Yang X 2011 *Phys. Lett. A* **375** 3978
[40] Ding C, Li J, Yang X, Zhang D and Xiong H 2011 *Phys. Rev. A* **84** 043840
[41] Ding C, Li J, Yang X, Zhan Z and Liu J B 2011 *J. Phys. B* **44** 145501
[42] Steck D 2010 ^{87}*Rb D line data* http://steck.us/alkalidata
[43] Yan M, Rickey E G and Zhu Y 2001 *J. Opt. Soc. Am. B* **18** 1057
[44] Jha P K, Rostovtsev Y V, Li H, Sautenkov V A and Scully M O 2011 *Phys. Rev. A* **83** 033404